

Can fully convolutional networks perform well for general image restoration problems?

Subhajit Chaudhury

Hiya Roy

s-chaudhury@ap.jp.nec.com
NEC Central Research Labs, Japan**

hiya.roy@ac.jaxa.jp
The University of Tokyo

Abstract. We present a fully convolutional network(FCN) based approach for color image restoration. Fully convolutional networks have recently shown remarkable performance for high level vision problems like semantic segmentation. In this paper, we investigate if fully convolutional networks can show promising performance for low level problems like image restoration as well. We propose a FCN model, that learns a direct end-to-end mapping between the corrupted images as input and the desired clean images as output. Experimental results show that our FCN model outperforms traditional sparse coding based methods and demonstrates competitive performance compared to the state-of-the-art methods for image denoising. We further show that our proposed model can solve the difficult problem of blind image inpainting and can produce reconstructed images of impressive visual quality.

1 Introduction

Image restoration is the technique to convert a noisy image into a clean, original one. The goal of image restoration is to reconstruct a plausible estimate of the original image from the noisy observation. Common image restoration problems are image denoising and image inpainting. Image denoising is the method of removing the external noise (usually modeled as additive white Gaussian noise) to obtain the original uncorrupted image. Such noise may arise while acquiring the image by electronic devices due to acquisition channel or some other external reasons. Another form of corruption for image signal occurs in the form of missing pixel values. Image inpainting is used for predicting such missing pixel values or removing sophisticated patterns like superimposed texts from images and preserve the original image information. In this paper, we focus on the problem of image denoising and blind image inpainting.

Image denoising is a well studied topic and various methods have been proposed to solve this problem. One approach for image denoising is to convert the image domain signal to a new domain representation[1, 2] and alter co-efficients in the transformed domain to produce the clean image. Other approaches for image denoising include modifications in the image domain itself. One notable

** The opinions expressed in this paper are solely of the author and do not represent the views of NEC Central Research Labs

technique in this category is total variation based image denoising [3]. This approach assumes that discrete image gradients in noisy image are larger than that in clean image and attempts to predict the clean image by solving a maximum-a-posteriori estimation problem with total variation as image prior. Image denoising by learning global image priors[4] is also a viable method.

Additionally, sparse coding based image denoising is a very popular technique which learns set of over-complete dictionaries from uncorrupted image patches and adapts to the noisy image at hand to produce the corresponding clean image. Such dictionary learning[5–7] based image denoising methods are shown to produce impressive performance which can also be extended to solve other image restoration tasks. With the availability of large datasets and efficient training platforms, recent works[8–10] in image denoising aim at learning direct mapping between noisy and clean image patches. Carefully engineered algorithms which exploit similarity in appearance of different patches[11–13] constitute the current state-of-the-art in image denoising. A notable work in this category is BM3D[11] and its color variant CBM3D[12].

Image inpainting can be broadly classified into two categories: non-blind inpainting and blind inpainting. While in non-blind inpainting, the algorithm is provided the prior knowledge of the spatial locations of the image with missing pixels or superimposed patterns that needs to be restored, blind inpainting methods aim to solve a much more challenging problem of simultaneously identifying and restoring the corrupted pixels. In the field of non-blind image inpainting, starting from the pioneering work of [14], region filling methods[15] have been proposed to obtain image inpainting. The Field-of-experts[4] model and the sparse coding based K-SVD[7] model are versatile models that can also be extended to perform non-blind inpainting. Blind inpainting on the other hand is a less mature field of study with limited implementations. To the best of our knowledge, SSDA based blind inpainting[10] is the most notable work in blind image inpainting for removing sophisticated superimposed patterns.

Sparse coding methods provide a unified framework[7] that can be adapted for both image denoising and inpainting tasks. Although sparse coding methods perform well for image restoration tasks, they share shallow learning structure. However recent research suggests that non-linear deep networks(MLP[8], Stacked Sparse Denoising Autoencoder[10]) can achieve superior performance in image restoration tasks. Dong et al. [16] showed that sparse coding based image super-resolution can be solved by convolutional networks.

Fully convolutional networks have shown promising performance for high level problems like segmentation[17]. In this paper, we propose a fully convolutional model for solving low-level image restoration problem. More specifically we solve the problems of image denoising(for additive white Gaussian noise) and blind inpainting based text removal and uniformly distributed missing pixel restoration. We argue that the proposed fully convolutional model performs restoration in 3 stages-(i)projecting overlapping image patches onto new bases (ii) Transforming the co-efficients of these bases to clean image co-efficients, and

(iii) Inverting the transformed co-efficients onto the image pixel space. Details on this can be found in section 2.2.

We perform supervised training on the proposed CNN architecture by presenting our network with noisy and clean image pairs. By noisy and clean pairs, we refer to the corrupted image and desired image after removing the noise. Our proposed model learns an end-to-end mapping between the noisy and the clean image. In recent years, CNN has gathered massive popularity because of its outstanding performance on various challenging visual classification tasks[18]. The reason behind this dramatic improvement in performance is attributed to the availability of huge training data[19] and availability of powerful GPUs for effective training. We also make use of these recent progresses for efficiently training deeper networks for color image restoration.

Contributions We present a multipurpose FCN model that can solve various image restoration problems for RGB images. Results in image denoising demonstrate that the proposed method is competitive with the state of the art methods. For image inpainting, although our model performs a much more difficult task of blind restoration, it demonstrates comparable visual reconstruction quality at par with non-blind inpainting methods. The capability of our model for blind inpainting of complex superimposed patterns is a major contribution of this paper.

2 Convolutional neural networks for Image Restoration

In this section we first formally define the problem of image restoration. A description on the network architecture of the proposed convolutional neural network is provided along with the details on the training procedure adopted for the network.

2.1 Problem formulation

Considering \mathbf{x} as the observed noisy image and \mathbf{y} as the clean image, the image corruption process is given by,

$$\mathbf{x} = g_\eta(\mathbf{y}) \quad (1)$$

where the function $g_\eta(\mathbf{y}) : \mathbb{R}^N \rightarrow \mathbb{R}^N$ is the corrupting process that produces the noisy image from the clean image. Both image denoising and inpainting processes can be explained by this framework.

For the task of image denoising, noisy image is obtained from the clean image by adding Gaussian noise. This can be expressed as,

$$\mathbf{x} = \mathbf{y} + \boldsymbol{\eta} \quad (2)$$

where each element of the additive noise $\eta_i \sim \mathcal{N}(0, \sigma)$. We assume that the noise is independent and identically distributed at each pixel. The task of image denoising is to predict the clean image \mathbf{y} given the noisy image \mathbf{x} .

For the task of image inpainting, the noisy image has missing pixel values(impulse noise) or superimposed patterns on the clean image. The noisy image, in this case, is obtained from the clean image by an element-wise multiplicative process. This can be expressed as,

$$\mathbf{x} = \mathbf{y} \odot \boldsymbol{\eta} \quad (3)$$

In this case, each element of noise η_i is a Bernoulli random variable taking values from $\{0, 1\}$. For the task of text removal, η is a structured noise which has a sophisticated pattern and the distribution of the noise cannot be explicitly formalized mathematically(since masking text have many possible variations). For restoring images which have random missing pixels, the empirical probability $P(\eta_i = 1) = 1 - \alpha$, where α is the fraction of missing pixels from the image.

2.2 Model description

Many traditional image restoration techniques perform domain transformation(like Fourier, Wavelets etc.) as the first step. Coefficients in the transformed domain are modified according to the task at hand. The modified co-efficients are then transformed back to the image domain to obtain the clean image by the inverting transform. Our proposed CNN model follows a similar intuition for image restoration.

- 1) *Projecting image patches onto learnt dictionary:* Traditional image restoration methods extract dense overlapping image patches and project them onto hand crafted[DCT, Haar] or pre-trained[PCA, K-SVD] bases. This operation can be performed by convolving the input image by a set of filters with spatial support equal to the patch size. For each such convolution we obtain a feature map. Formally, the i^{th} feature map in the first layer is represented as:

$$\mathbf{O}_1(i) = \max(0, W_1(i) * \mathbf{x} + B_1) \quad (4)$$

where $W_1(i)$ and B_1 represent the i^{th} filter and bias in the 1^{th} layer. For color image input, each of the filters have spatial support of $3 \times f_1 \times f_1$ where f_1 is the size of overlapping patches in the first layer. For each of the n_1 number of filters in the first layer, we obtain a basis onto which the image patch is projected by convolution. $\text{ReLU}(\max(0, x))$ is used as the activation function in this layer.

- 2) *Non-linear transformation:* After projecting the overlapping image patches onto learned dictionaries in the first layer, these co-efficients are mapped onto a new representation by a non-linear transformation. The non-linear transformation is modeled to have two parts: (a) Pixel-wise co-efficient transformation (b) Neighborhood based co-efficient transformation.

$$\hat{\mathbf{O}}_{l-1} = \psi_v(O_1)\psi_e(O_1) \quad (5)$$

where $\psi_v(\cdot)$ models the pixel-wise co-efficient transformation which is achieved by convolution kernels of size 1×1 . $\psi_e(\cdot)$ models interaction of the neighboring co-efficients around a pixel which is achieved by convolution kernel of size greater than 1. The non-linearity in this stage is achieved by consecutive convolution operations followed by ReLU[20] activation.

- 3) *Reconstruction by weighted averaging:* The co-efficients obtained from the non-linearity transform is projected onto the bases representing the corresponding clean image patch and weighted average is performed on overlapping patches to form the final clean image. This operation can be formally represented as:

$$\hat{Y} = \max(0, W_l * O_{l-1} + B_l) \quad (6)$$

where \hat{Y} is the predicted clean RGB image. Each filter in the last layer W_l has spatial support of size $n_{l-1} \times f_l \times f_l$. For color image restoration problem the number of filters in the last layer is 3, corresponding to RGB channels of the image. The convolutional filters in the last layer projects the co-efficients obtained from non-linearity transform onto the clean image dictionary and performs weighted averaging to construct the clean image.

Since each of these operations can be performed by convolution operation, the mapping described above can be represented as a convolutional neural network. This CNN will consist of only convolution layers, the weights and biases for each of which will be optimized by looking at noisy/clean image pairs using standard back-propagation algorithm to minimize mean squared error. For the above mentioned pipeline, operation 1 is performed by the first layer and operation 3 is performed by the last layer. The intermediate layers are responsible for non-linear mapping of co-efficients.

2.3 Network architecture details

Based on the above mention description, we describe two architectures for Image Restoration by Convolutional Neural Networks(**IRCNN**) in color images.

- 1) ***IRCNN-1(9-5-1-5)***: It is a 4 layered CNN consisting of only convolution layers(+ReLU non-linearity). Figure 1(a) shows details on filter weights and number of convolution parameters for each layer. The pixel-wise co-efficient transformation is achieved by convolution kernels of size 1×1 and interaction with the neighboring co-efficients around a pixel which is achieved by convolution kernel of size 5.
- 2) ***IRCNN-2(5-5-1-5-5-5)***: Recent research[21, 8, 10] suggests that increasing the depth of CNN architecture moderately can produce superior performance. Following that, we also used a deeper network architecture with 6 convolution layers using same design strategies as IRCNN-1. Figure 1(b) shows details on this CNN architecture. We found that increasing depth, improves performance and convergence rates for image denoising problem. Since this architecture gives superior performance in image denoising, we train only this model for solving blind image inpainting tasks(IRCNN-1 is not trained for in-painting operation).

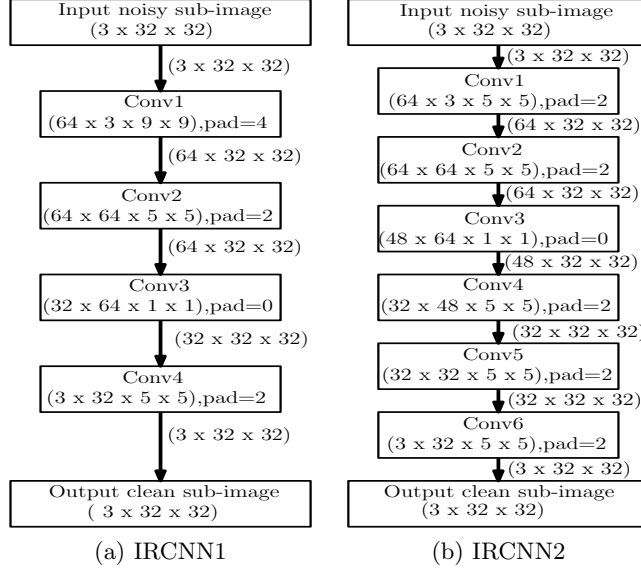


Fig. 1: Image Restoration CNN(IRCNN) architectures. Each conv layer has ReLU non-linearity

2.4 Training

Our CNN model learns end-to-end mapping between the input noisy images and the output clean images. We optimize the network parameters $\Theta = \{W_i, B_i\}$, $i = \{1, 2, \dots, l\}$ by minimizing the loss between the set of clean images $\{\mathbf{Y}_i\}$ and images predicted $\{\hat{\mathbf{Y}}_i\}$ from the noisy image set $\{\mathbf{X}_i\}$. Let us define this overall mapping as $\hat{\mathbf{Y}}_i = F(\mathbf{X}_i, \Theta)$. Then the optimal parameters are obtained as,

$$\hat{\Theta} = \arg \min_{\Theta} \frac{1}{n} \sum_{i=1}^n \|F(\mathbf{X}_i, \Theta) - \mathbf{Y}_i\|_2^2 \quad (7)$$

where n is the number of images used for training the network. Minimizing the mean squared error between the clean and predicted image is performed by randomly sampling some smaller images from the clean/noisy images. Some pre-processing is done on these "sub-images" in the form of mean subtraction and normalization. In order for the size of the input and output sub-image to be same, we perform padded convolution in each layer. In our implementation, we used $3 \times 32 \times 32$ sized sub-images. For each kind of noise we produce the noisy image from the clean image and sample the same spatial location on each of these image pairs to produce a clean/noisy sub-image pairs.

The mean square error was minimized using standard mini-batch gradient descent with momentum update. We use constant learning rate for all the layers. We start with learning rate of 0.05 and after each complete pass over the training

data decrease it linearly to reach the final value of 10^{-4} . Momentum is varied from initial value of 0.9 to 0.999. We implemented our model using Theano[22, 23] library in Python.

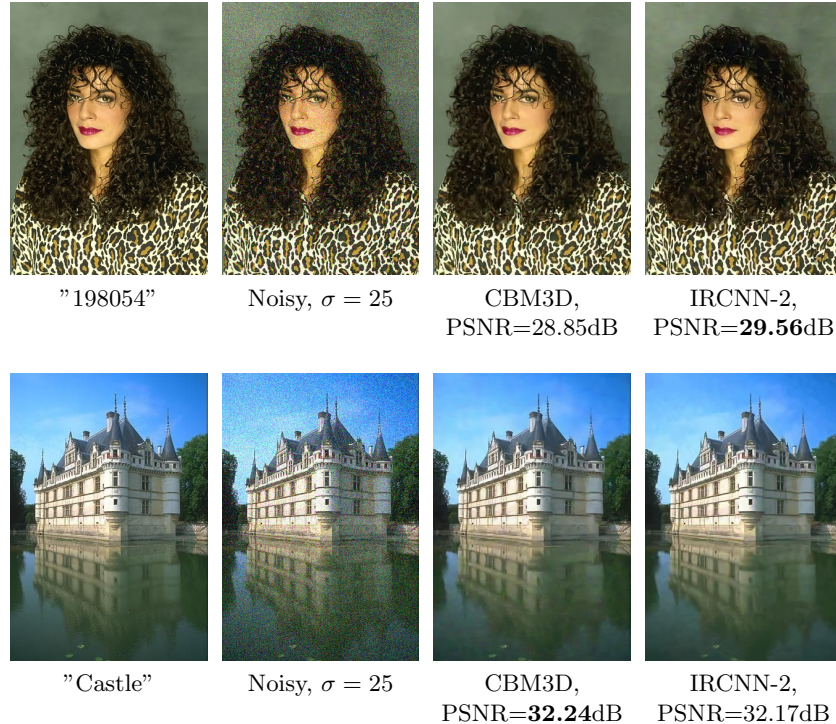


Fig. 2: Image denoising results on Berkeley segmentation dataset

3 Experimental Results

In this section we describe the experiments that we performed for evaluating our model’s performance. Detailed explanation on the datasets that were used for model training and testing are provided. Procedures for noisy/clean image pair extraction for each task is described. We investigate the performance of our proposed network on different datasets and produce a comparison to state-of-the-art techniques. For quantitative evaluation, we compare the PSNR values obtained by each method. A discussion on the filters learned by our approach is also provided.

3.1 Image denoising

Noisy images are created by corrupting clean images with additive white Gaussian noise. For our experiments we trained our network for noise levels of $\sigma = 25$ and $\sigma = 50$. For training we extract sub-image pairs from original clean/noisy image pairs and train our network on these sub-image pairs.

Training data: For training our network we use data from two datasets:(1) Image-Net[19] (2) MSCOCO [24]. We randomly choose 6000 image from each of the two datasets and corrupt each image with additive white Gaussian noise. From each such image pair, we choose 16 randomly samples of size $3 \times 32 \times 32$, giving a total of 192,000 sub-image pairs. Training is done following standard mini-batch gradient descent approach(batch-size=256) with momentum update. It took 4 days to train the network on a modern GPU during which time 4000 passes over all the 192,000 sub-images were performed for IRCNN-2 network. Both IRCNN-1 and IRCNN-2 architectures were trained for $\sigma = 25$ and only IRCNN-2 was trained for $\sigma = 50$.

| Image | $\sigma = 25$ | | | | $\sigma = 50$ | |
|----------|---------------|--------------|---------|--------------|---------------|--------------|
| | KSVD | CBM3D | IRCNN-1 | IRCNN-2 | CBM3D | IRCNN-2 |
| Castle | 31.19 | 32.24 | 31.91 | 32.17 | 28.67 | 28.66 |
| Mushroom | 30.26 | 31.20 | 30.92 | 30.92 | 27.77 | 27.60 |
| Horse | 29.81 | 30.67 | 30.62 | 30.83 | 27.59 | 27.84 |
| Kangaroo | 28.39 | 29.19 | 29.19 | 29.30 | 26.37 | 26.45 |
| Train | 28.16 | 28.72 | 28.80 | 28.88 | 24.52 | 25.06 |
| Average | 29.56 | 30.40 | 30.29 | 30.42 | 26.98 | 27.12 |

Table 1: Image denoising performance for Berkeley segmentation dataset images

Testing data: Testing is performed by sliding window technique and averaging overlapping reconstructions. We define two test-sets for evaluating our performance:

- 1) Berkeley segmentation dataset[25]: We test our algorithm on selected images from this dataset-”castle”, ”mushroom”, ”horse”, ”train” and ”kangaroo”, which are used to compare our performance with K-SVD[7] and CBM3D[12] methods for image denoising.
- 2) Pascal VOC 2012[26]: 500 images were randomly selected from this dataset and the performance was compared with state of the art CBM3D[12] method for image denoising.

We choose the sparse-coding based image denoising method(K-SVD) from [7] as our baseline for comparing denoising performance. Images from the Berkeley segmentation dataset, used in [7], were used to compare the performance of

IRCNN-1 and IRCNN-2 with baseline method K-SVD[7] and CBM3D[12], a state-of-the-art color image denoising method. For each image, experiments were performed 10 times and the average PSNR value was reported. we used PSNR values reported by the authors in [7] for the comparison. For CBM3D, we used the Matlab code provided by the authors for our evaluations. Table 1 shows the comparison of performance for image denoising with $\sigma = 25$ and $\sigma = 50$. On this small testing dataset, IRCNN-2 produces superior performance for 3 out of 5 images(for both $\sigma = 25$ and $\sigma = 50$) and has the best overall performance outperforming both sparse coding based KSVD method state-of-the-art CBM3D method. Figure 2 show the qualitative comparison for image denoising on this small dataset images.

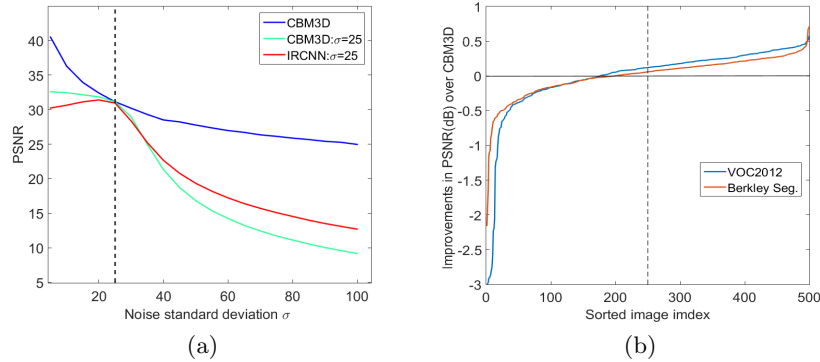


Fig. 3: (a) Comparison of IRCNN-2 for $\sigma = 25$ at other noise levels with CBM3D. (b) Improvements of our method compared to CBM3D on two larger datasets for image denoising.

For a more comprehensive comparison with CBM3D method, we tested the performance of both the methods on two larger datasets of 500 images from Berkeley segmentation dataset[25] and Pascal VOC 2012[26] dataset. For each image in the dataset, experiments were performed 5 times and the average value was used. Improvements in PSNR achieved by our method, compared to CBM3D for $\sigma = 25$ on both datasets is shown in figure 3(b). The comparisons between the CBM3D and IRCNN-2 is shown in Table 2. These quantitative results demonstrate that the proposed IRCNN model(IRCNN-2) performs at-par with(often better than) state-of-the-art denoising methods.

We further perform additional evaluations where we test the learned IRCNN-2 model trained at $\sigma = 25$ for various other noise levels and plot the PSNR performance. The plot at various noise levels for the image "mushroom" is shown in figure 3(a) which shows that our learned model produces competitive performance compared to CMB3D at $\sigma = 25$ but performance deteriorates for other

| | CBM3D | IRCNN-2 | Percentage better than CBM3D |
|------------|--------------|--------------|------------------------------|
| Berkeley | 30.89 | 30.90 | 60% |
| PASCAL VOC | 30.79 | 30.78 | 65% |

Table 2: Image denoising performance for 500 images from Berkeley and PASCAL VOC dataset. The table shows mean PSNR values for CBM3D and IRCNN-2 and percentage of images for which IRCNN-2 performed better than CBM3D.

noise levels. To compare with similar effects in CBM3D, we fixed the input parameter to $\sigma = 25$ for CBM3D. Similar performance is seen for CBM3D algorithm with knowledge of $\sigma = 25$, although our learned network performs slightly better at higher noise levels. CBM3D provided with correct noise information produces superior performance which is understandable.

3.2 Blind image inpainting

We perform image inpainting task for two kinds of corruption: (1) Images are corrupted with i.i.d. uniformly distributed missing pixels (2) Image are superimposed with complicated patterns like text. In blind inpainting, the prior knowledge on the spatial location of the missing pixels are not provided which makes it a difficult problem. The training data for blind inpainting was same as that for image denoising. We make no attempt to change the network architecture for this task and perform training on IRCNN-2 model.

3.2.1 Missing pixel inpainting Noisy images were created by randomly assigning 80% of the pixel values in each channel as zeros and then 192,000 sub-images(similar to denoise case) were created by randomly sampling 16 images from each clean/noisy image pair. Similar to the denoising case, training is done following standard mini-batch gradient descent approach taking took 4 days to train the network for 4000 passes over the entire training dataset.

For 80% missing pixel case we obtain as PSNR performance of 28.74dB for the image "castle" from berkeley segmentation dataset. The best reconstruction performance of 29.65dB reported in [7] by non-blind K-SVD inpainting technique. Our model has a lower PSNR performance compared to K-SVD because we solve a more difficult task of blind inpainting where the location of the missing pixels are unknown compared to non-blind case where the information about the location of the missing pixel simplifies the inpainting problem to a large extent.

Qualitatively our model shows good reconstruction quality, as seen from the reconstruction results in figure 4. For the castle image, the reconstructed image is visually similar to the original clean image. For the "relativity"¹image, we observe that, while the text in the noisy image is not at all clearly visible, the image predicted by our model successfully restores readability for moderately large

¹ Image obtained from Google Images(keyword:"relativity paper"), labeled for non-commercial reuse with modification

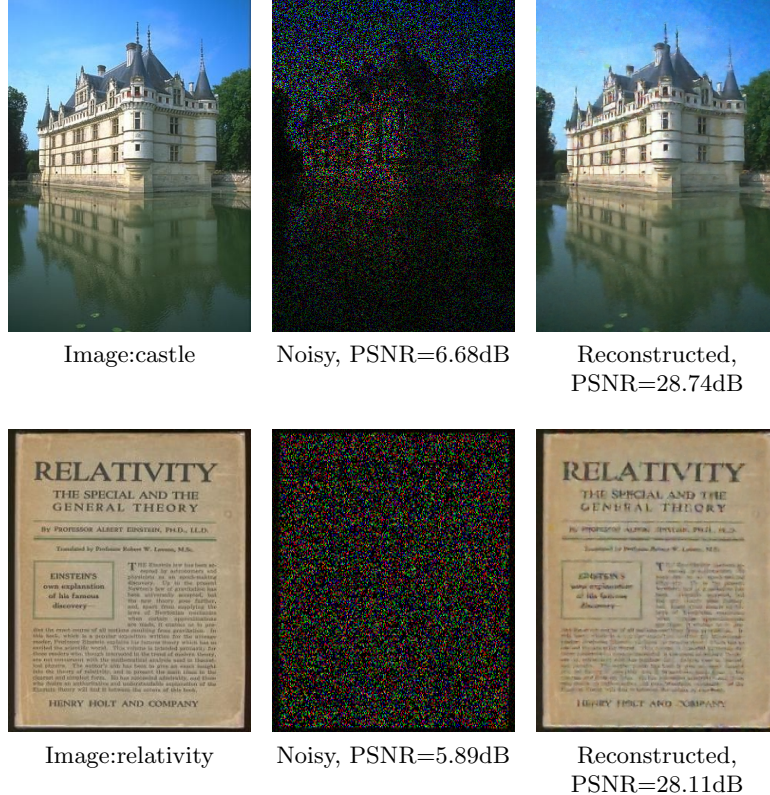


Fig. 4: Missing pixel inpainting results on various images by IRCNN-2

text. These qualitative and quantitative results demonstrate the effectiveness of our model for missing pixel restoration.

3.2.2 Text removal For text removal problem, noisy images were created by super-imposing random texts on the clean images from 15 different font-styles and font-size varying from 15pix to 25pix. Following similar methodology as previous methods, we create 192,000 sub-images by randomly sampling 16 images from each clean/noisy pair and training is done following standard mini-batch gradient descent with similar parameters as mentioned for previous tasks. Interestingly, we observed our model does not differentiate between the various tasks(denoising or inpainting) it is learning and takes almost similar time for learning direct mapping between input and output in each case.

We tested the performance of our algorithm of the classic image used in the original inpainting paper[14] for text removal. Quantitative evaluation on the data revealed that our model obtained a PSNR value of 30.95dB. For lack of blind inpainting methods, we compare our performance with non-blind inpaint-

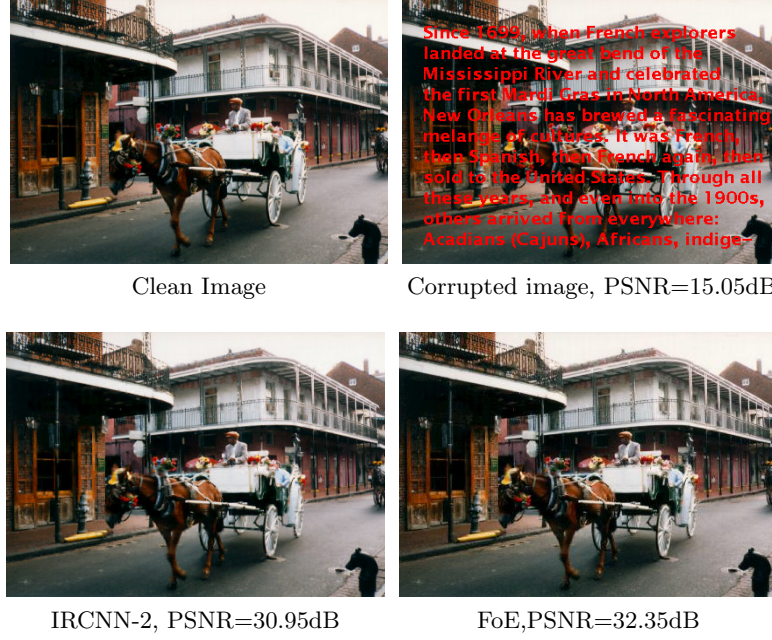


Fig. 5: Comparison of superimposed text removal performance

ing method of Field-of-Experts(FoE) model[4] and K-SVD model[7]. For this image, FoE achieves PSNR value of 32.35dB while K-SVD(as reported in [7]) achieves 32.45dB. We used the Matlab code provided by the authors, for evaluating the performance using FOE model. The time required by FoE for text removal was 584 seconds (using $24 \times 5 \times 5$ filters) while IRCNN-2 took 5.6 seconds for the same task.

Quantitative evaluations reveal that although we solve a much difficult blind text-removal problem we achieve PSNR performance close to non-blind inpainting methods. Qualitative evaluations(figure 5) reveal some discrepancies in connectivity of edges and some blurring effects on locations where the text was superimposed in the noisy image. However compared to the results in [10], where a shadowy artifact of the superimposed text(which could be identified as text) remained on the final reconstructed image, our model can completely remove texts in the final image with no serious text artifacts. The capability of our method for blind inpainting of complicated superimposed texts is a notable contribution of this paper.

3.3 Visualizing learned filters

The first layer of the proposed model learns a set of dictionaries which projects the input noisy image patch onto a new representation space. Figure 6 (a) shows

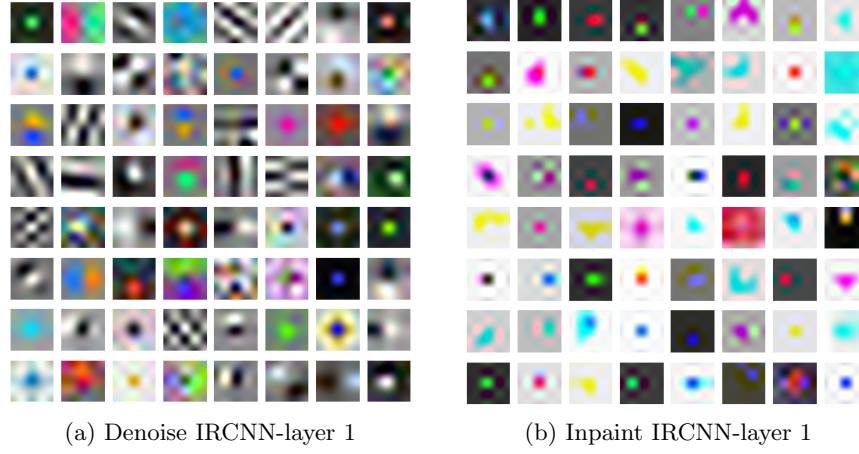


Fig. 6: Learned filter weights in the first layer for IRCNN

the first layer filters of size $64 \times 5 \times 5$ (scaled to intensity 0-255) for IRCNN-2 architecture for denoising operation($\sigma = 25$) learned from the training data described in section 3.1. Each of the filters have learned a specific functionality like oriented edge detectors, Gabor-like filters, Haar and DCT like kernels and are visually very similar to dictionaries learned by traditional sparse coding based methods.

Interestingly, almost 50% of the filters have gray-scale appearances which implies that they do not exploit cross-channel correlation while the other filters do use correlations between RGB channels. This suggests that performance of color image denoising can be improved by modeling dependencies between RGB channels than simply denoising each channel separately and combining the results.

Figure 6 (b) shows the first layer filters of size $64 \times 5 \times 5$ for IRCNN-2 architecture for the task of predicting missing pixels(randomly chosen 80% pixels missing). These filters are not easily interpretable and we are currently conducting studies to learn what functionalities these learned filters depict. However these filters are much more colored than those for the case of denoising which suggests that these filters strongly model RGB channel correlations for predicting missing pixels values.

4 Conclusion

We have presented a fully convolutional deep learning approach for image restoration of RGB images. The proposed approach learns an end-to-end mapping between noisy and clean image patches. Experimental evaluations on image denoising show that fully convolutional image denoising demonstrates competitive

performance with the state-of-the-art methods. For image inpainting, our model solves the difficult problem of blind inpainting and successfully removes i.i.d. uniformly distributed impulse noise as well as sophisticated patterns like text with impressive visual quality of reconstruction. These results show that fully convolutional networks can indeed provide a good model for low level image restoration problems. In addition to the demonstrated competitive accuracy, the proposed FCN based image restoration model is light-weight and feed-forward in structure which can be readily implemented in practical systems.

References

1. Luisier, F., Blu, T., Unser, M.: A new sure approach to image denoising: Interscale orthonormal wavelet thresholding. *IEEE Transactions on Image Processing* **16** (2007) 593–606
2. Portilla, J., Strela, V., Wainwright, M.J., Simoncelli, E.P.: Image denoising using scale mixtures of gaussians in the wavelet domain. *IEEE Transactions on Image Processing* **12** (2003) 1338–1351
3. Rudin, L.I., Osher, S., Fatemi, E.: Nonlinear total variation based noise removal algorithms. *Phys. D* **60** (1992) 259–268
4. Roth, S., Black, M.J.: Fields of experts: a framework for learning image priors. In: 2005 IEEE Computer Society Conference on Computer Vision and Pattern Recognition (CVPR’05). Volume 2. (2005) 860–867 vol. 2
5. Aharon, M., Elad, M., Bruckstein, A.: k -svd: An algorithm for designing over-complete dictionaries for sparse representation. *IEEE Transactions on Signal Processing* **54** (2006) 4311–4322
6. Elad, M., Aharon, M.: Image denoising via sparse and redundant representations over learned dictionaries. *IEEE Transactions on Image Processing* **15** (2006) 3736–3745
7. Mairal, J., Elad, M., Sapiro, G.: Sparse representation for color image restoration. *IEEE Transactions on Image Processing* **17** (2008) 53–69
8. Burger, H.C., Schuler, C.J., Harmeling, S.: Image denoising: Can plain neural networks compete with bm3d? In: Computer Vision and Pattern Recognition (CVPR), 2012 IEEE Conference on. (2012) 2392–2399
9. Jain, V., Seung, S.: Natural image denoising with convolutional networks. In Koller, D., Schuurmans, D., Bengio, Y., Bottou, L., eds.: Advances in Neural Information Processing Systems 21. Curran Associates, Inc. (2009) 769–776
10. Xie, J., Xu, L., Chen, E.: Image denoising and inpainting with deep neural networks. In Pereira, F., Burges, C.J.C., Bottou, L., Weinberger, K.Q., eds.: Advances in Neural Information Processing Systems 25. Curran Associates, Inc. (2012) 341–349
11. Dabov, K., Foi, A., Katkovnik, V., Egiazarian, K.: Image denoising by sparse 3-d transform-domain collaborative filtering. *IEEE Transactions on Image Processing* **16** (2007) 2080–2095
12. Dabov, K., Foi, A., Katkovnik, V., Egiazarian, K.: Color image denoising via sparse 3d collaborative filtering with grouping constraint in luminance-chrominance space. In: 2007 IEEE International Conference on Image Processing. Volume 1. (2007) I – 313–I – 316
13. Ram, I., Elad, M., Cohen, I.: Image processing using smooth ordering of its patches. *IEEE Transactions on Image Processing* **22** (2013) 2764–2774

14. Bertalmio, M., Sapiro, G., Caselles, V., Ballester, C.: Image inpainting. In: Proceedings of the 27th Annual Conference on Computer Graphics and Interactive Techniques. SIGGRAPH '00, New York, NY, USA, ACM Press/Addison-Wesley Publishing Co. (2000) 417–424
15. Criminisi, A., Perez, P., Toyama, K.: Region filling and object removal by exemplar-based image inpainting. *IEEE Transactions on Image Processing* **13** (2004) 1200–1212
16. Dong, C., Loy, C.C., He, K., Tang, X.: Image super-resolution using deep convolutional networks. *IEEE Transactions on Pattern Analysis and Machine Intelligence* **38** (2016) 295–307
17. Long, J., Shelhamer, E., Darrell, T.: Fully convolutional networks for semantic segmentation. In: 2015 IEEE Conference on Computer Vision and Pattern Recognition (CVPR). (2015) 3431–3440
18. Krizhevsky, A., Sutskever, I., Hinton, G.E.: Imagenet classification with deep convolutional neural networks. In Pereira, F., Burges, C.J.C., Bottou, L., Weinberger, K.Q., eds.: *Advances in Neural Information Processing Systems 25*. Curran Associates, Inc. (2012) 1097–1105
19. Deng, J., Dong, W., Socher, R., Li, L.J., Li, K., Fei-Fei, L.: ImageNet: A Large-Scale Hierarchical Image Database. In: CVPR09. (2009)
20. Nair, V., Hinton, G.E.: Rectified linear units improve restricted boltzmann machines. In Frnkranz, J., Joachims, T., eds.: *Proceedings of the 27th International Conference on Machine Learning (ICML-10)*, Omnipress (2010) 807–814
21. He, K., Zhang, X., Ren, S., Sun, J.: Delving deep into rectifiers: Surpassing human-level performance on imagenet classification. In: 2015 IEEE International Conference on Computer Vision (ICCV). (2015) 1026–1034
22. Bergstra, J., Breuleux, O., Bastien, F., Lamblin, P., Pascanu, R., Desjardins, G., Turian, J., Warde-Farley, D., Bengio, Y.: Theano: a CPU and GPU math expression compiler. In: *Proceedings of the Python for Scientific Computing Conference (SciPy)*. (2010) Oral Presentation.
23. Bastien, F., Lamblin, P., Pascanu, R., Bergstra, J., Goodfellow, I.J., Bergeron, A., Bouchard, N., Bengio, Y.: Theano: new features and speed improvements. *Deep Learning and Unsupervised Feature Learning NIPS 2012 Workshop* (2012)
24. Lin, T.Y., Maire, M., Belongie, S., Hays, J., Perona, P., Ramanan, D., Dollár, P., Zitnick, C.L.: Microsoft COCO: Common Objects in Context. In: *Computer Vision – ECCV 2014: 13th European Conference, Zurich, Switzerland, September 6-12, 2014, Proceedings, Part V*. Springer International Publishing, Cham (2014) 740–755
25. Martin, D., Fowlkes, C., Tal, D., Malik, J.: A database of human segmented natural images and its application to evaluating segmentation algorithms and measuring ecological statistics. In: *Proc. 8th Int'l Conf. Computer Vision. Volume 2*. (2001) 416–423
26. Everingham, M., Eslami, S.M.A., Van Gool, L., Williams, C.K.I., Winn, J., Zisserman, A.: The pascal visual object classes challenge: A retrospective. *International Journal of Computer Vision* **111** (2015) 98–136